Radar-Based Human Gait Recognition in Cane-Assisted Walks

Ann-Kathrin Seifert, Abdelhak M. Zoubir

Signal Processing Group

Technische Universität Darmstadt, 64283 Darmstadt, Germany

Email: {seifert, zoubir}@spg.tu-darmstadt.de

Moeness G. Amin

Center for Advanced Communications

Villanova University, Villanova, PA 19085 USA

Email: moeness.amin@villanova.edu

Abstract—**Radar technology for in-home gait assessment has recently become of increased interest due to its safety, reliability and privacy-preserving, non-wearable sensing mode. Radar-based micro-Doppler signatures of humans can be used to reveal key characteristics that capture changes in gait and enable detecting abnormalities. In elderly care, the influence of assistive walking devices on gait time-frequency signal characteristics has to be examined for proper diagnoses, assessment of rehabilitations, and fall risk predictions. In this paper, we demonstrate the effects of assistive walking devices, such as a cane, on the back-scattered radar signals. A K-band radar is used to discriminate between assisted and unassisted walks. Detection of walking aids and gait recognition are performed based on features obtained from the cadence-velocity diagram. Experimental data are presented for walking towards and away from radar, delineating different micro-Doppler signatures which are attributed to distinctions in upper and lower leg kinematics in both cases.**

I. Introduction

A great number of seniors resort to assistive walking devices, such as a cane or a walker, to compensate for decrements in balance, gain mobility and to overcome the fear of falling. In 2011, 8.5 million U.S. seniors aged 65 and older reported having any assistive walking device, with the most commonly device being a cane used by two thirds of the elderly [1]. The correct use of mobility devices is essential to guarantee optimal support and avoid postural deformities. This becomes important in both cases of elderly gaining mobility and patients recovering from injuries or physical impairment. However, assessing proper handling of walking aids is often difficult for healthcare providers and nursing staff. The information provided by the monitoring radar on elderly's use of a cane inside his/her home, day and night, can be valuable in designing proper treatment and charting a recovery course. Further, constant monitoring of changes in gait enables early diagnosis of different diseases, such as Parkinson's, cardiopathies and strokes [2]. Obviously, the performance of such gait monitoring systems should not be impaired by the use of walking aids.

Due to its unobstrusive, safe and privacy-preserving operating mode, radar for indoor human monitoring is promising to become a leading technology for assisted living in the future [3], [4]. From the back-scattered radar signal, human activities can be recognized by exploiting time-frequency features caused by the micro-Doppler (mD) effect [5]. The so-called mD signatures occur as modulations around the carrier frequency of the transmitted radar signal in the Doppler domain and are characteristic for targets' motions. Specifically, in the case of a walking human, the mD signatures describe human kinematics by capturing velocity, acceleration, and rotation of individual body parts. Hence, mD features are well suited to discriminate different human motions and recognize variations in these.

Radar-based human gait recognition has been previously investigated, e.g. in [6], [7], [8]. However, so far, human gait characteristics with assistive walking devices have not been widely examined. Amin *et al.* [9], [10] showed that walking aids, such as a cane or a walker, can be detected by carefully analyzing the back-scattered radar signal. For discriminating between gaits with and without a cane, two features were extracted from the time-frequency representation (TFR) utilizing the extended modified B-distribution (EMBD). The work by Gurbuz *et al.* [11] investigated the effect of various walking aids on the characteristics of radar return signatures of human walk. Different degrees of mobility were compared, i.e., an unaided walk, limping, walking with a cane/tripod or a walker, and using a wheelchair. Amongst other systems, a 24 GHz pulse-Doppler radar was used for gait classification utilizing pseudo-Zernike moments, as suggested in [12], and a support vector machine. Using measurements of 5 s (and 10 s) duration a classification accuracy of 72.6% (79.7%) was achieved, respectively. For the unaided walk, the correct classification rate was 73.3% (81.3%), whereas the use of a cane was correctly detected in 55.4% (61.9%) of the cases.

This work focuses on cane-assistive walks and examines corresponding changes in gait patterns and their effect on the characteristics of radar mD signatures. First, we call attention to the fundamental differences in mD signatures of walks towards and away from the radar system. These differences have been overlooked and not considered by any existing work in this field. Then, the aim is to discern an unassisted walk from a walk with a cane, independent on how the cane is actually used. In particular, we consider assisted walks where the cane is synchronized with the opposite or the same side leg as the arm carrying the cane, as well as, walks where the cane is synchronized with neither leg.

The remainder of this paper is organized as follows. Section II introduces time-frequency and cadence-velocity analysis of back-scattered radar signals from walking humans. From the cadence-velocity representation features are extracted for classification of normal and cane-assisted walks, as described in Section III. Experimental results using real data are presented in Section IV and final conclusions are given in Section V.
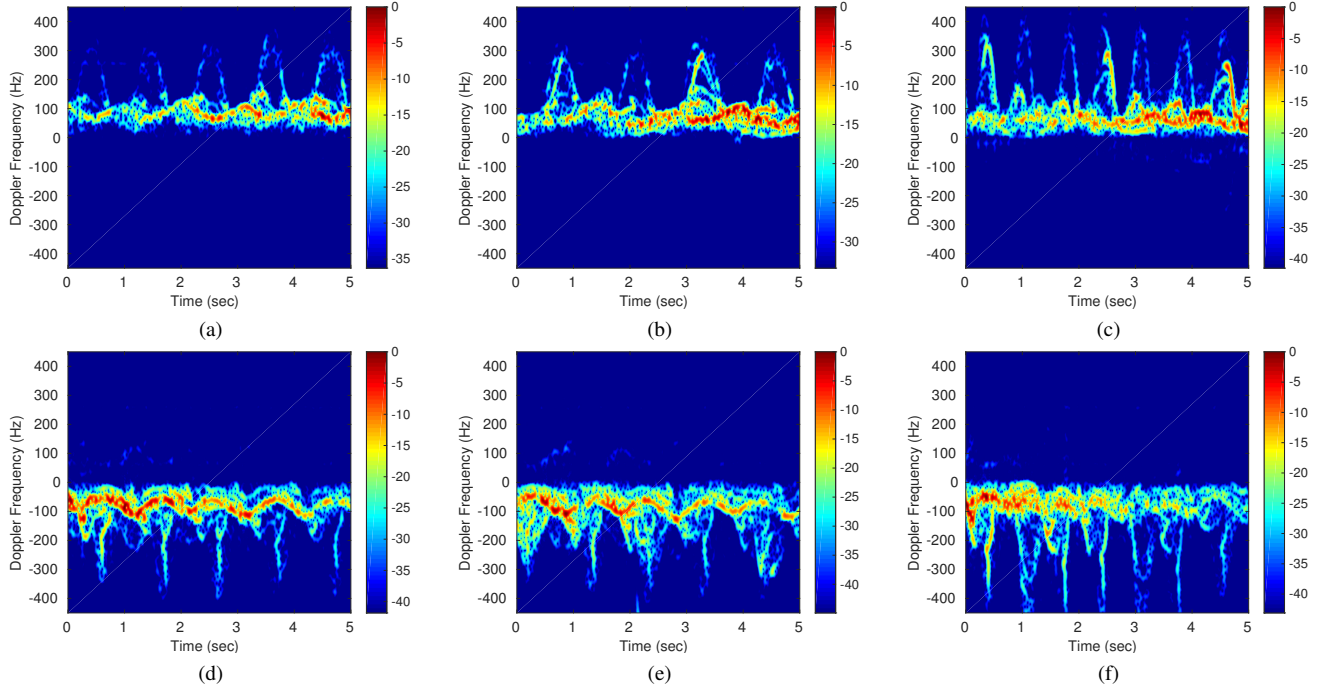
Fig. 1: Examples of spectrograms for a person (a) walking slowly towards the radar, (b) with a cane in sync with one leg, and (c) with a cane out of sync with any leg (cane‑leg‑leg‑cane‑...). For walking away from the radar system, (d) shows an unassisted walk, in (e) the pattern is (cane‑leg‑cane‑leg‑cane), and in (f) it is (leg‑cane‑leg‑leg‑cane‑...).

II. GAIT CHARACTERISTICS WITH AND WITHOUT CANE

A. Time-Frequency Representations

The back-scattered radar signal from a walking person is highly non-stationary and consists of multiple superimposing components. TFRs are well suited for revealing the time-varying characteristics of the received radar signal in the joint Doppler frequency vs. time domain. The most common choice of TFR in this area is the spectrogram, which belongs to the class of non-linear TFRs and depicts how the signal power varies with time and frequency [3]. The spectrogram is given by the squared magnitude of the short-time Fourier transform and is calculated as

$$S(n,k) = \left| \sum_{m=0}^{M-1} w(m)x(n-m)e^{-j2\pi \frac{mk}{M}} \right|^2, n = 0, \ldots, N-1,$$
(1)

where $w(\cdot)$ is a window of length $M \in \mathbb{N}$, $x(\cdot)$ is the time-domain radar return signal of length $N \in \mathbb{N}$, and k is the normalized frequency.

The use of assistive walking devices leads to distinct mD signatures compared to an unassisted walk. Fig. 1 depicts examples of spectrograms for different walking styles with and without a cane when moving towards (top row) and away from (bottom row) the radar system. In (a), the spectrogram of a person walking slowly towards the radar is given. The swinging of the feet leads to clear sinusoidal-shaped mD stride signatures around the main torso signature. The latter can be identified by the highest energy in the spectrogram. Note that there is no arm swinging involved in all measurements presented here. Fig. 1 (b) and (c) show spectrograms of a person walking with a cane. In (c), the cane is moved in sync with the opposite-side leg such that the first and third mD signature depict the overlay of foot and cane signatures. In (c), the cane is moved asynchronously with the legs, which leads to non-overlapping foot and cane mD signatures. Here, the first, fourth, and seventh mD signature are due to the cane movement, whereas the remainders are normal stride signatures as in (a).

For the same walking styles, Fig. 1 (d), (e) and (f) show the spectrograms when the radar system has a back-view. Clearly, the mD signatures are different compared to towards-radar measurements. In (d), we see that an mD signature of a normal gait stride is composed of two major parts: a sinusoidal-shaped and an impulsive-like mD component. The former is due to the pendulum-like motion of the thigh swinging forward. The latter is caused by reflections from the upper calf. Its salient mD signature is embraced in the barely recognizable sinusoidal-shaped foot signature. This means that the upper and lower leg kinematics in a human walk lead to distinct mD features when the radar has a back view compared to front-view measurements. These characteristics are also visible in every second stride signature in (e), which shows a person walking with a cane being moved in sync with one leg. Knowing the salient features of a normal gait stride signature, we can visually tell that the second and fourth mD signature correspond to a normal stride, whereas the remaining ones are altered by the cane's movement. Finally, (f) shows the spectrogram of a cane-assisted walk away from the radar, where the cane is moved out of sync with any leg. Thereby, distinct mD signatures of cane and leg become visible. Here, the second and fifth mD signature come from the cane only, whereas the remaining ones correspond to a normal stride.
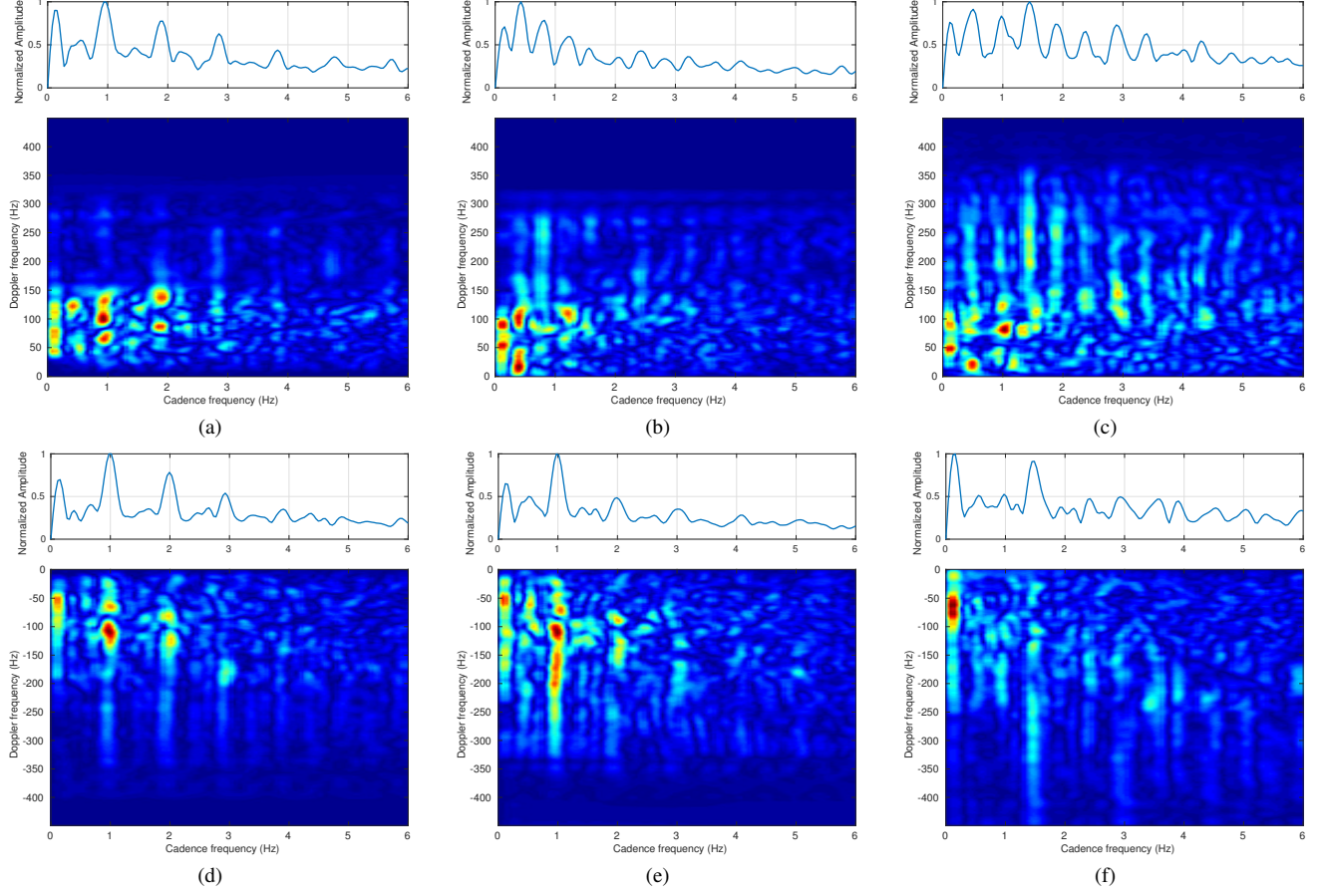
Fig. 2: Examples of cadence-velocity diagram (CVD) (bottom) and mean cadence frequency spectrum (top) corresponding to the measurements in Figure 1, i.e., the top row depicts measurements towards the radar system and bottom row shows measurements when the radar has a back-view.

B. Cadence-Velocity Diagram Analysis

The human walk is periodic with each stride or half of the gait cycle. As described in section II-A, the use of an assistive walking device, such as a cane, alters the mD gait signature in the TFR. In order to analyze periodicities in the spectrogram, we calculate the cadence-velocity diagram (CVD). Features obtained from the cadence-velocity (CV) domain have been employed previously for radar-based human motion classification, e.g., in [6], [12], [13], [14]. The CVD is obtained by taking the Fourier transform of the spectrogram along the time dimension, i.e., Doppler frequency slices are transformed to the cadence frequency domain. Thus, the CVD is calculated using the spectrogram $S(n,k)$ as

$$C(\varepsilon, k) = \mathcal{F}_n\{S(n,k)\} = \left| \sum_{n=0}^{N-1} S(n,k)e^{-j2\pi\frac{\varepsilon n}{N}} \right|, \quad (2)$$

where ε denotes the cadence frequency and $N \in \mathbb{N}$ is the number of samples in a frequency slice of the spectrogram.

For a walking person, the CVD reveals the mean velocity along with the step rate in a joint Doppler frequency vs. cadence frequency representation. Summing over all cadence frequencies for each Doppler frequency gives the mean Doppler spectrum. The maximum of the mean Doppler spectrum serves

as an estimate of the average walking speed of a person, also referred to as base velocity. Taking the sum over all Doppler frequencies for each cadence frequency, yields the mean cadence spectrum. The cadence frequency that corresponds to the highest amplitude in the mean cadence spectrum, is the fundamental cadence frequency, which corresponds to the stride rate in unassisted walks. However, for assisted walks, this correspondence is not necessarily true, as explained below.

Fig. 2 shows the CVDs of the walks given in Fig. 1. For an unassisted walk, the CVD is depicted in (a), where $0.98\,\text{Hz}$ is the fundamental cadence frequency and represents the stride rate of the walk. When walking with a cane in sync with one leg, every other mD signature is altered. This results in an additional peak in the mean cadence spectrum at half the stride rate. E.g., from the CVD in (b), we find that the stride rate is $0.78\,\text{Hz}$ due to corresponding high amplitudes in the range of $120 - 270\,\text{Hz}$ in Doppler frequency. However, the highest peak in the mean cadence spectrum appears at half the stride rate. The latter comprises both, the cane's movement of high Doppler frequencies and the arm movements of lower Doppler frequencies. Similarly, walking with a cane that is aligned with neither leg leads to a specific pattern in the CVD, as depicted in (c). In this case, the mean cadence spectrum peaks at $1.48\,\text{Hz}$, which describes the rate of adjacent mD signatures in the TFR.

The CVD clearly shows an additional peak at one third of the fundamental cadence frequency. It relates to the similarity of every third mD signature, which is either pairs of cane or leg signatures. Moreover, we observe a strong harmonic at two thirds of the fundamental cadence frequency. Note, that we cannot define a stride rate here, as the strides are nonperiodic.

Fig. 2 (d), (e) and (f) show the corresponding CVDs for walking away from the radar with and without a cane. In general, the mean cadence spectra reveal stronger peaks at the fundamental cadence frequency compared to towards-radar measurements. However, the effects of the cane on the CVD structure are less prominent.

III. Gait Classification in Cane-assisted Walks

A. Cadence-Velocity Features

In order to perform classification of different human walking styles, both assisted and unassisted, we extract classical gait features from the CV domain [6], [13]. First, the mean cadence spectrum is formed from the CVD. In this case, only absolute Doppler frequencies larger than $150\,\mathrm{Hz}$ are considered to confine the feature to leg and cane movements only. The highest peak in the mean cadence spectrum marks the fundamental cadence frequency. Further, to capture the profile of the mean cadence spectrum, we extract its dominant peaks and calculate the mean peak distance in cadence frequency. Finally, the base velocity is estimated from the maximum in the mean Doppler spectrum. Thus, we define a feature vector for each measurement as

$$\mathbf{f} = [f_0, \bar{d}_{\mathrm{pks}}, v_0]^T, \tag{3}$$

where f_0 is the fundamental cadence frequency, $\bar{d}_{\mathrm{pks}}$ is the average distance of detected peaks in the mean cadence spectrum and v_0 is the estimated base velocity of the walk.

B. Principal Component Analysis of CVDs

Besides utilizing CV features that have a physical interpretation, such as the average stride rate and the base velocity, the CVD itself exhibits characteristic patterns for identifying different walking styles, as outlined in Section II-B. In order to exploit these patterns for gait classification and detection of a cane, we perform a principal component analysis (PCA) of the CVDs. A similar approach, i.e., PCA of spectrograms, has been successfully applied to radar-based human gait recognition [15], [16] and fall motion detection [17]. However, for gait recognition the CVD is more appropriate for revealing the periodicity of each of the micro-Doppler components.

The CVD is obtained as follows. First, we calculate the spectrogram of a 6 s measurement sampled at 2.56 kHz. Here, the STFT is calculated using a Hamming window of length 255 samples, which is equivalent to 0.1 s, and 2048 frequency bins. Thus, the spectrogram is given on a grid of 2048 Doppler frequency bins by 15,360 time samples. Then, the FT of the spectrogram is taken along the time axis to yield the CVD. Using 2^{16} points in the FT calculation leads to a cadence frequency resolution of approximately $0.02\,\mathrm{Hz}$. In order to compensate for different stride rates among the measurements, we use f_0 to warp the CVD image along the cadence frequency axis, such that all CVDs have $f_0 = 1\,\mathrm{Hz}$. Then, we normalize each CVD by scaling its entries to the range of $[0, 1]$ such

that it becomes a gray-scale image. Then, we extract the relevant part, i.e., Doppler frequencies from $0\,\mathrm{Hz}$ to $+450\,\mathrm{Hz}$ and $-450\,\mathrm{Hz}$ for towards and away from radar measurements, respectively, and cadence frequencies up to 3 Hz. As we expect stride rates around 1 Hz the latter range is sufficiently large to capture the fundamental cadence and its first and second harmonic. Given this excerpt of the CVD the resulting image is of dimension 361×78 pixels.

For PCA we form a data matrix whose columns contain all vectorized CVD-images that are in the training set. The vectorized CVD-images are of size 28158×1, where the length of the vector describes the dimensionality of our vector space. Note, that we arrange the CVD-images row by row to the 1D vector to take into account the relations of a given pixel to pixels in neighboring columns, which is more appropriate in our case. Performing PCA on the $i \times j$ data matrix, composed of j vectorized CVD images with $i = 28158$ pixels, we obtain j eigenvectors of length i, actually eigenimages, and j corresponding eigenvalues. Principal components are those eigenvalues that explain most of the variance in the data. The eigenimages that correspond to the principal components span a subspace. All CVD images are projected on this subspace and the projections, denoted as $\mathbf{p}$, are used for classification. Choosing l principal components, the feature vector is thus defined as

$$\mathbf{p} = [p_1, p_2, \ldots, p_l]^T, \quad l \leq j \in \mathbb{N}. \tag{4}$$

C. Classification

Next, a classifier $C(\cdot)$ is used to map the final feature vector, formed of feature vectors defined in (3) and (4), as

$$\mathbf{z} = [\mathbf{f}, \mathbf{p}]^T, \tag{5}$$

on a discrete set of classes $c = C(\mathbf{z})$, $c \in \{\mathcal{C}_1, \mathcal{C}_2, \ldots, \mathcal{C}_q\}$, where $\mathcal{C}$ denotes a single class and q is the number of classes. Here, we aim at distinguishing between an unassisted (NW) and an assisted walk, whereby the latter can be a walk with a cane in sync with either leg (CW) or out of sync with any leg (CW/oos). Thus, we define $q = 3$ classes such that $c \in \{\mathrm{NW}, \mathrm{CW}, \mathrm{CW/oos}\}$. Here, the nearest neighbor (NN) classifier is used to discriminate between unassisted and two types of assisted walks, as this method of supervised learning method typically achieves high classification performance without a priori assumptions on the distribution from which the training samples were generated. The classifier is trained on a subset of the available data, whereas the remainder is used for testing. Unseen test data is then classified based on the distance to the nearest training case. Here, the Euclidean distance measure is used.

IV. Experimental results

A. Experimental Setup

The UWB radar [18] data were mostly collected in a semi-controlled lab environment at the Radar Imaging Lab at Villanova University. About one third of the data were collected in an office environment at Technische Universität Darmstadt. The radar was set to FMCW mode with linear frequency modulation sweeps and a carrier frequency of 24 GHz. Doppler filtering was applied to obtain the velocity information of the target by utilizing the phase shift between different sweeps. In

TABLE I: Walking styles being analyzed and corresponding number of measurements.

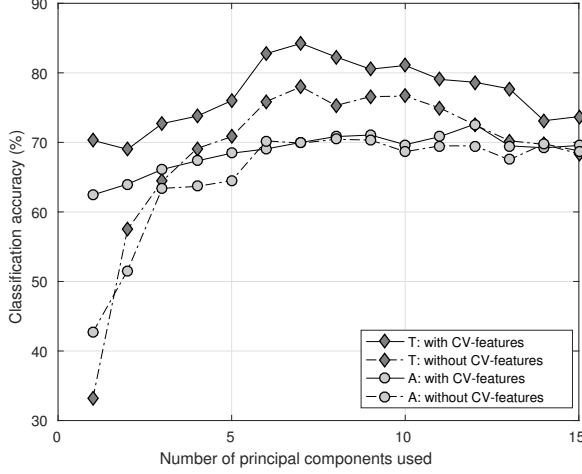| Walking style	Towards	Away
Normal walk (NW)	17	22
Cane-assisted walk - synchronized (CW)	25	23
Cane-assisted walk - out of sync (CW/oos)	13	12
Total	55	57

Fig. 3: Classification accuracy vs. the number of principle components used for towards (T) and away (A) from radar measurements.

total, seven subjects were asked to walk slowly back and forth between two points in front of the radar, approximately 4.5 m and 1 m from the antenna feed point, which was positioned 1.15 m above the floor. Data were collected with a non-oblique view to the targets and at a $0°$ angle relative to the radar line-of-sight. All subjects were asked not to swing their arms. In total, a set of 112 measurements of 6 s duration are considered, whereof 55 are towards the radar and 57 are away from the radar. The details of the test set are given in Table I.

B. Feature Selection

The performance of the classifier is sensitive to the number of features used as well as to the direction of motion, i.e., towards or away from the radar. Figure 3 gives the classification accuracy in dependence of the number of principle components used, where the dashed lines refer to a reduced feature vector with PCA-based features only. Here, the classification accuracy is given by the number of correct classifications divided by the total number of samples in the test set. In general, classification accuracy is higher when including the CV-based features, particularly in case of towards-radar measurements. Concluding, we choose a number of seven eigenimages for both directions, and include the CV-based features for classification.

C. Classification Results

Classification is performed for towards and away from radar measurements separately. In each case, 70% of the data are randomly chosen for training and the remainder

TABLE II: Confusion matrix for towards-radar measurements with (and without) CV-based features. Numbers represent the correct classification rate in %.

True class / Predicted class	NW	CW	CW/oos
Normal walk (NW)	**83 (76)**	14 (22)	3 (2)
Cane-assisted walk - synchronized (CW)	12 (13)	**86 (85)**	2 (2)
Cane-assisted walk - out of sync (CW/oos)	1 (5)	16 (28)	**83 (67)**

TABLE III: Confusion matrix for away-from-radar measurements with (and without) CV-based features. Numbers represent the correct classification rate in %.

True class / Predicted class	NW	CW	CW/oos
Normal walk (NW)	**63 (72)**	34 (27)	3 (1)
Cane-assisted walk - synchronized (CW)	27 (30)	**71 (68)**	2 (2)
Cane-assisted walk - out of sync (CW/oos)	6 (16)	7 (17)	**87 (67)**

are used for testing. Final results, see Table II, are obtained by averaging 100 classification results. Towards radar walks can be classified correctly in 84% of the cases using PCA-based features and CV features. The false alarm (FA) rate as well as the missed detection (MD) rate are both 17%. Here, MD refers to the case where a cane was present, but the gait is wrongly classified as unassisted. Without CV features the classification accuracy decreases to 76% (FA: 24%, MD: 20%). For measurements of a human walking away from the radar system, classification accuracy is 70% (FA: 34%, MD: 34%), using PCA-based features and CV features. Without CV features, the classification accuracy drops to 68% (FA: 28%, MD: 36%).

For both directions, mostly walks with a cane in sync with one leg (CW) are confused with an unassisted walk (NW) and vice-versa. Considering that we only evaluated measurements of 6 s duration, this result is not unexpected, as the cane only shows 2-3 times during a measurement, depending on the stride rate. For longer observation times, this confusion should decrease. Further, in view of the variability of walks considered here, i.e., walks with different base velocities and stride rates, as well as different persons walking, the results underscore the applicability of the presented approach.

V. CONCLUSION

This work deals with human gait recognition in cane-assisted walks, which contributes to the subject of assisted living and gait analysis for diagnoses, rehabilitations, and fall risk prediction in elderly care. The influence of assistive walking devices on radar-based human walk characteristics is revealed. Features for gait classification in cane-assisted walks are extracted from CVDs of back-scattered radar data utilizing PCA. Using real data obtained with a K-band radar, gait classification results are presented for the two cases of moving towards and away from the radar with and without a cane.

REFERENCES

[1] N. M. Gell, R. B. Wallace, A. Z. Lacroix, T. M. Mroz, and K. V. Patel, "Mobility device use in older adults and incidence of falls and worry about falling: Findings from the 2011–2012 national health and aging trends study," *J. of the Amer. Geriatrics Soc.*, vol. 63, no. 5, pp. 853–859, 2015.

[2] A. Muro-de-la Herran, B. Garcia-Zapirain, and A. Mendez-Zorrilla, "Gait analysis methods: An overview of wearable and non-wearable systems, highlighting clinical applications," *Sensors*, vol. 14, no. 2, pp. 3362–3394, 2014.

[3] M. G. Amin, Y. D. Zhang, F. Ahmad, and K. C. D. Ho, "Radar signal processing for elderly fall detection: The future for in-home monitoring," *IEEE Signal Process. Mag.*, vol. 33, no. 2, pp. 71–80, 2016.

[4] V. C. Chen, D. Tahmoush, and W. J. Miceli, Eds., *Radar Micro-Doppler Signatures: Processing and Applications*, Institution of Engineering and Technology, 2014.

[5] V. C. Chen, *The micro-Doppler effect in radar*, Artech House, 2011.

[6] M. Otero, "Application of a continuous wave radar for human gait recognition," in *SPIE Defense + Security*, 2005, pp. 538–548.

[7] I. Orović, S. Stanković, and M. Amin, "A new approach for classification of human gait based on time-frequency feature representations," *Signal Processing*, vol. 91, no. 6, pp. 1448–1456, 2011.

[8] F. Wang, M. Skubic, M. Rantz, and P. E. Cuddihy, "Quantitative gait measurement with pulse-Doppler radar for passive in-home gait assessment," *IEEE Trans. Biomed. Eng.*, vol. 61, no. 9, pp. 2434–2443, 2014.

[9] M. G. Amin, F. Ahmad, Y. D. Zhang, and B. Boashash, "Micro-Doppler characteristics of elderly gait patterns with walking aids," in *SPIE Defense + Security*, 2015, pp. 94611A–94611A.

[10] M. G. Amin, F. Ahmad, Y. D. Zhang, and B. Boashash, "Human gait recognition with cane assistive device using quadratic time-frequency distributions," *IET Radar, Sonar & Navigation*, vol. 9, no. 9, pp. 1224–1230, 2015.

[11] S. Gurbuz, C. Clemente, A. Balleri, and J. Soraghan, "Micro-Doppler based in-home aided and un-aided walking recognition with multiple radar and sonar systems," *IET Radar, Sonar & Navigation*, 2016.

[12] C. Clemente, L. Pallotta, A. D. Maio, J. J. Soraghan, and A. Farina, "A novel algorithm for radar classification based on Doppler characteristics exploiting orthogonal Pseudo-Zernike polynomials," *IEEE Trans. Aerosp. Electron. Syst.*, vol. 51, no. 1, pp. 417–430, 2015.

[13] S. Björklund, H. Petersson, and G. Hendeby, "Features for micro-Doppler based activity classification," *IET Radar, Sonar & Navigation*, vol. 9, no. 9, pp. 1181–1187, 2015.

[14] S. Björklund, T. Johansson, and H. Petersson, "Evaluation of a micro-Doppler classification method on mm-wave data," in *2012 IEEE Radar Conf.*, 2012, pp. 0934–0939.

[15] B. G. Mobasseri and M. G. Amin, "A time-frequency classifier for human gait recognition," in *SPIE Defense, Security, and Sensing*, 2009, pp. 730628–730628.

[16] F. H. C. Tivive, S. L. Phung, and A. Bouzerdoum, "Classification of micro-Doppler signatures of human motions using log-Gabor filters," *IET Radar, Sonar & Navigation*, vol. 9, no. 9, pp. 1188–1195, 2015.

[17] B. Jokanović, M. Amin, and F. Ahmad, "Radar fall motion detection using deep learning," in *2016 IEEE Radar Conf.*, 2016.

[18] Ancortek Inc., "SDR-KIT 2500B," http://ancortek.com/sdr-kit-2500b, retrieved: 09/11/2016.